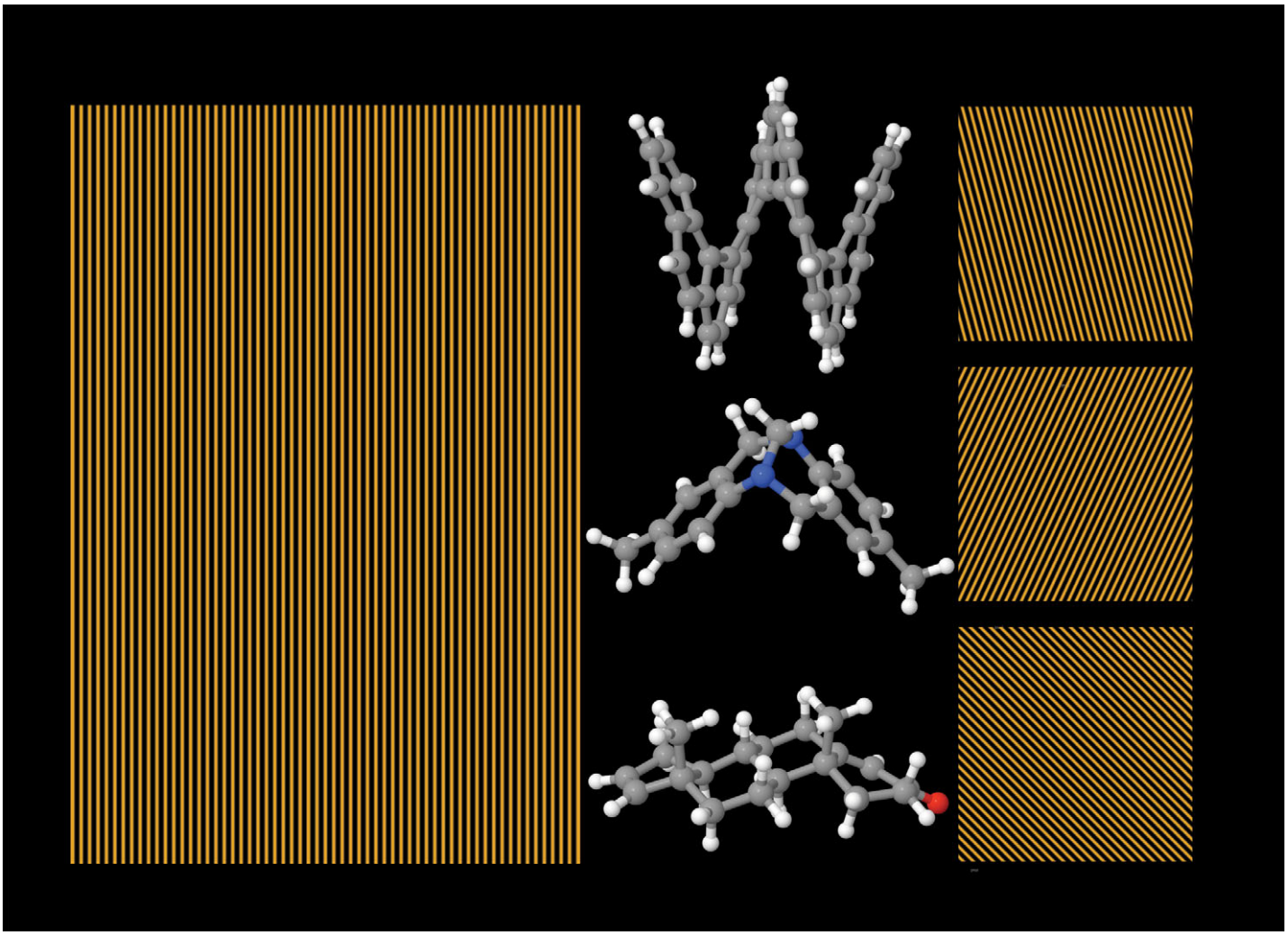


Showcasing research from the Centre for Theoretical and Computational Chemistry, University of Tromsø, Norway, and the Center for Theoretical Chemistry, University of Bochum, Germany.

Title: Optical rotation calculations on large molecules using the approximate coupled cluster model CC2 and the resolution-of-the-identity approximation

The article investigates the accuracy of the approximated second-order coupled cluster model CC2 for the calculation of optical rotations of molecules with up to 72 atoms. The CC2 results are shown to be less scattered compared to experiment than the DFT results. CC2 calculations show in particular significant improvements over DFT for molecules that are strongly influenced by weak intramolecular interactions.

As featured in:



See Friese *et al.*, *Phys. Chem. Chem. Phys.*, 2014, **16**, 5942.

ROYAL SOCIETY OF CHEMISTRY

www.rsc.org/pccp

Registered charity number: 207890

PCCP

PAPER

View Article Online
View Journal | View Issue

Published on 09 January 2014. Downloaded by Ruhr Universitat Bochum on 07/07/2014 13:19:21.

Cite this: *Phys. Chem. Chem. Phys.*, 2014, **16**, 5942

Optical rotation calculations on large molecules using the approximate coupled cluster model CC2 and the resolution-of-the-identity approximation

Daniel H. Friese*[a] and Christof Hättig[b]

Received 14th October 2013,
Accepted 27th November 2013

DOI: 10.1039/c3cp54338b

www.rsc.org/pccp

We investigate the performance of the approximate coupled cluster singles- and doubles model CC2 in the prediction of optical rotations of organic molecules. For this purpose we employ a combination of two test sets from the literature which include small and medium-sized rigid organic molecules and a series of helicenes. CC2 calculations on molecules as large as 11-helicene became possible through a recent implementation of frequency-dependent second-order properties for CC2 which makes use of the resolution-of-the-identity approximation for the electron repulsion integrals. The results are assessed with respect to the accuracy of the absolute values of the optical rotation and the prediction of the correct sign, which is crucial for the determination of absolute configurations. The performance of CC2 is compared with that of density functional theory at the B3LYP and CAM-B3LYP levels. Furthermore we investigated the influence of the molecular geometry and the one-electron basis set and tested to which extent spin-component scaling changes the results.

1 Introduction

During the last two decades the interest in quantum chemical calculations of optical rotations (OR) has increased significantly. A reason for this is the applicability of such calculations to determine absolute configurations (AC) by comparison of experimental and calculated values. Although the comparison of calculated and measured vibrational CD spectra has proven to be more reliable,[1] comparison of optical rotations is very useful since this quantity is very easy to measure. Therefore there is a remarkable interest in reliable techniques for calculations of the optical rotation especially of biologically relevant large organic molecules.

The first theoretical studies in this field were presented by Cheeseman *et al.* in 2000 for Hartree–Fock (HF) and density functional theory (DFT).[2] Due to the size of the molecules which are typically of interest computational efficiency is an important requirement for the applicability of a method for such calculations. Another requirement is the reliability of AC determination which has been investigated *e.g.* in ref. 3. Since the balance between reliability and efficiency has been considered to be good for DFT, it has become a standard method for the prediction of optical rotations for organic molecules as shown by a large amount of older[4,5] but also recent studies.[6]

The use of correlated wave function based methods for OR calculations is hampered by the lack of origin invariance which generally occurs in calculations of frequency dependent magnetic properties.[7] While for DFT and HF calculations this problem can be solved using so-called London orbitals, also known as gauge including atomic orbitals (GIAOs),[8,9] this technique cannot be used with correlated wave function based methods which describe the wave function response with unrelaxed orbitals.[10–13] The first very easy approach to tackle this problem was to use the center of mass of the molecule as the origin of the coordinate system.[14] Nevertheless real origin invariance in coupled cluster calculations of optical rotations can be realized by using the so-called modified velocity gauge formulation by Pedersen *et al.* which is also employed in our present study.[7]

In Pedersen's work the approximate coupled cluster singles and doubles model CC2 has been used for OR calculations of some small molecules.[7,15] The CC2 model was introduced by Christiansen[16] and has proven to be very reliable for the calculation of excitation energies[17] as well as ground- and excited state molecular properties.[15,18,19] Especially the frequency dependence of properties is described well by CC2[20,21] since it predicts the poles (*i.e.* excitation energies) with a similar accuracy as CCSD. However even if the problem of gauge invariance is solved, the applicability of correlated wave function based methods suffers from their high computational costs. Since the CC2 implementation in TURBOMOLE, which takes benefit of the RI-approximation for the two-electron integrals, has recently been extended to second derivatives of energy,[21,22] this method

[a] *Centre for Theoretical and Computational Chemistry, Department of Chemistry, University of Tromsø, N-9037 Tromsø, Norway. E-mail: daniel.h.friese@uit.no*
[b] *Lehrstuhl für Theoretische Chemie, Ruhr-Universität Bochum, D-44801 Bochum, Germany. E-mail: christof.haettig@rub.de*

This journal is © the Owner Societies 2014

Published on 09 January 2014. Downloaded by Ruhr Universitat Bochum on 07/07/2014 13:19:21.

can now be applied for the calculation of frequency-dependent second-order properties of considerably larger molecules. In this study we combine the RI-CC2 approach with Pedersen's technique from ref. 7 to realize fast and origin-independent correlated wave function based calculations on optical rotations. The reliability of CC2 for a large test set of "real life molecules" is assessed in this work with focus on the prediction of the correct sign and the magnitude of the optical rotation in comparison to experimental data. Furthermore we investigate the importance of basis set effects and the influence of spin-scaling techniques. For this assessment a test set is used which is based on two test sets from the literature. Additionally we studied a series of helicene molecules as large-scale applications do demonstrate how the RI-CC2 implementation extends the applicability of CC2 towards larger molecules.

2 Theory

The optical rotation is related to the trace of the electric dipole–magnetic dipole polarizability tensor at the frequency of the incident light. Thus any implementation of frequency-dependent second-order molecular properties can in principle be used for calculations on the optical rotation if origin invariance can be realized.

The specific rotation, which is given in units of deg (dm g cm^{-3})$^{-1}$, can be obtained from

$$[\alpha] = 28\,800\pi^2 N_A a_0{}^4 \frac{\nu}{M}\beta(\omega), \quad (1)$$

where N_A is Avogadro's number and $a_0{}^4$ the Bohr radius in cm. ω is the frequency of light in atomic units and ν is the same in cm^{-1}. Following ref. 23 β is obtained from the trace of the optical rotation tensor η as

$$\beta(\omega) = -\mathrm{Re}\frac{\mathrm{Tr}\left\langle\!\left\langle \vec{p}, \vec{L} \right\rangle\!\right\rangle_\omega}{6\omega^2} \quad (2)$$

where $\vec{L}$ is the angular momentum operator and $\vec{p}$ is the velocity representation of the dipole moment operator. To obtain origin invariance we use the modified velocity gauge expression for β proposed by Pedersen:[7]

$$\beta_{\mathrm{mod}}(\omega) = -\mathrm{Re}\frac{\mathrm{Tr}\left\langle\!\left\langle \vec{p}, \vec{L} \right\rangle\!\right\rangle_\omega - \left\langle\!\left\langle \vec{p}, \vec{L} \right\rangle\!\right\rangle_0}{6\omega^2}, \quad (3)$$

where $\left\langle\!\left\langle \vec{p}, \vec{L} \right\rangle\!\right\rangle_0$ are the elements of the optical rotation tensor at frequency 0 which is an unphysical static contribution to the optical rotation. It is purely an artifact of approximations, *e.g.* the incomplete one- and many-electron basis sets, and has to be removed[7] from $\left\langle\!\left\langle \vec{p}, \vec{L} \right\rangle\!\right\rangle_\omega$. $\beta_{\mathrm{mod}}(\omega)$ is then used instead of $\beta(\omega)$ in eqn (1).

3 Computational details

3.1 Methods and basis sets

The tensor elements of $\left\langle\!\left\langle \vec{p}, \vec{L} \right\rangle\!\right\rangle$ were calculated with our implementation of analytic second derivatives of energy for RI-CC2[21] in TURBOMOLE[24] which has been reported recently. Augmented Dunning-style basis sets[25,26] have been used in the calculations as detailed below. For the RI approximation of the two-electron repulsion integrals we used the corresponding optimized auxiliary basis sets.[27,28] For calculations on molecules containing bromine effective core potentials have been used for all 1s-, 2s- and 2p-electrons.[29] In all other cases we used the frozen-core approximation for all non-valence electrons in the correlation and response treatment.

We computed the optical rotation for a test set of 50 molecules taken from published test sets and in addition to the 8-, 9-, 10- and 11-helicenes. For the calculations on the helicenes with eight rings or more a recently completed MPI-parallel version of the code for second derivatives with RI-CC2 has been used.

For all molecules of the test set the calculations were done for $[\alpha]$ at 589 nm since for all molecules experimental values for the optical rotation at this wavelength were available which were all measured in the condensed phase.

3.2 The test set

42 molecules were taken from the OR45 test set by Srebro *et al.* which was set up for the validation of density functionals for OR calculations.[6] The test set consists of 42 organic molecules and three transition metal complexes. The latter were not considered here to circumvent multireference problems. The organic molecules include tricycles, quadricycles, terpenoids, a steroid and helicene derivatives with up to 48 atoms. 8 additional molecules were taken from a test set proposed by Crawford *et al.* which consists of rigid cyclic terpenoids and an adamantane derivative and were originally used for the comparison of coupled cluster and DFT results.[30] Five molecules are contained in both test sets.

In the test set of Srebro *et al.* the geometries of all molecules were optimized using B3LYP and the 6-311G(d,p) basis set while in Crawford's work B3LYP and 6-31G* were used for the geometry optimizations. The 42 structures from Srebro's work have been used by us with both the original geometries and geometries optimized with MP2 in the cc-pVTZ basis set. The eight structures from Crawford's test set were used in B3LYP/6-31G* and MP2/cc-pVTZ optimized geometries. About half of the molecules considered here are also contained in the large test set of Stephens *et al.* which was used to evaluate the reliability of AC determination.[3]

For the evaluation of our results we considered it to be useful to split the molecules of our test set into groups according to the size and structure:

- 13 *tricycles*, structures are given in Fig. 1
- 9 *norbornane derivatives*, structures are given in Fig. 2
- 6 *pinene derivatives*, structures are given in Fig. 3
- 7 *large molecules* (with more than 35 atoms), structures are given in Fig. 4
- 15 *miscellaneous molecules*, structures are given in Fig. 5

4 Results and discussion

The results from our calculations are listed in Table 1 in comparison with experimental results (references for the experimental values given therein) and the theoretical results of Crawford[30] and Srebro.[6] A summary of the comparison is shown in Fig. 6 where for specific

Published on 09 January 2014. Downloaded by Ruhr Universitat Bochum on 07/07/2014 13:19:21.

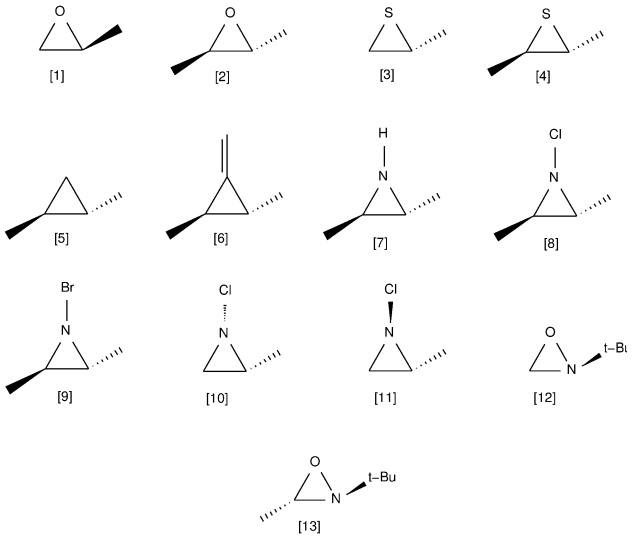


Fig. 1 Tricyclic molecules of the test set.

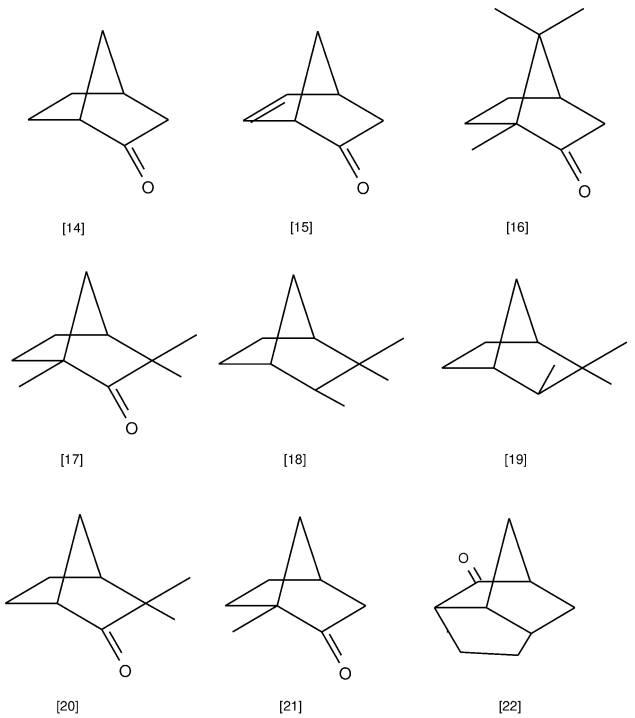


Fig. 2 Norbornane derivatives from the test set.

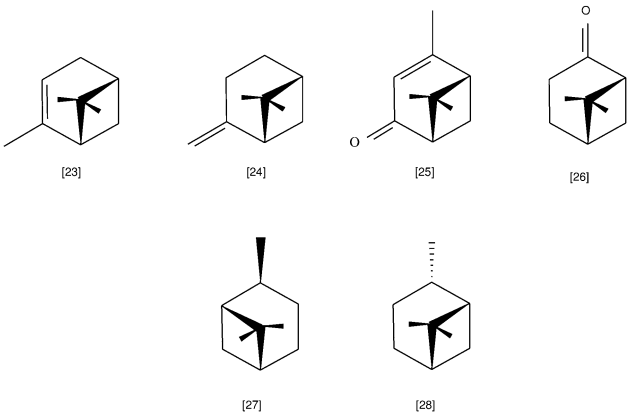


Fig. 3 Pinene derivatives from the test set.

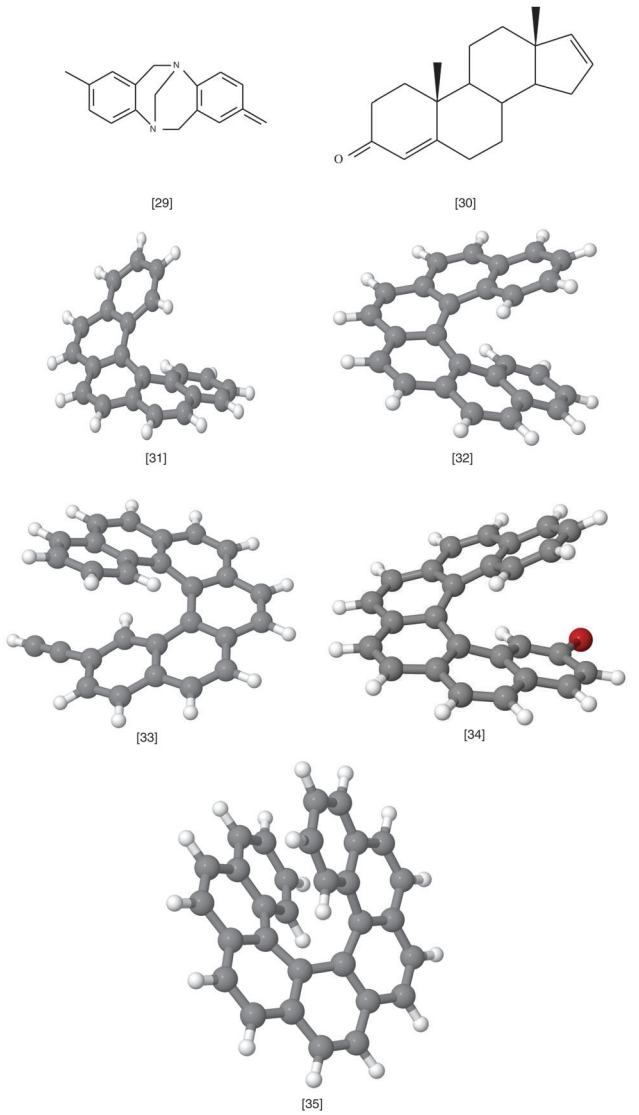


Fig. 4 Large molecules from the test set.

rotations between −190 and 220 deg (dm g cm^{-3})$^{-1}$ the results from B3LYP, CAM-B3LYP and CC2 are plotted with the corresponding experimental values as abscissa. This plot covers 42 of the 50 molecules of our test set. Only the helicene derivatives (**31–35**), norbornenone (**15**), the steroid (**30**), and cyclooctene (**49**) have been excluded because of their high optical rotations.

Comparing experimental and calculated values we note that for 13 molecules the reproduction of the experimental values by theoretical calculations is very difficult. In these cases the experimental and theoretical results differ by a factor of two or more although the theoretical results from the various methods are very similar (**6, 9, 12, 13, 14, 18, 21, 24, 26, 27, 28, 39,** and **50**). We suspect that these molecules are largely influenced by solvent effects.

 This journal is © the Owner Societies 2014

Published on 09 January 2014. Downloaded by Ruhr Universitat Bochum on 07/07/2014 13:19:21.

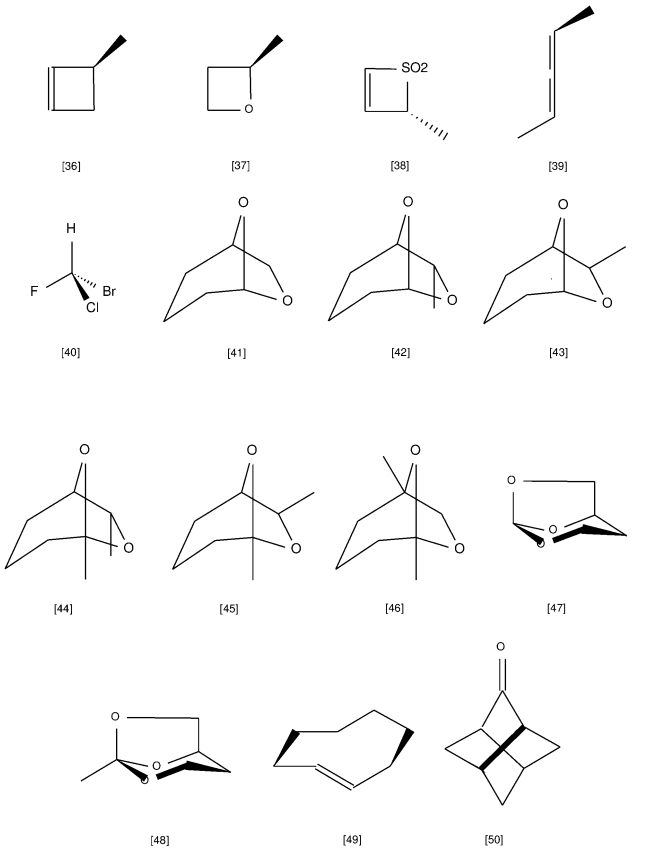


Fig. 5 Miscellaneous molecules from the test set.

For some of the problematic molecules Mort *et al.* have also found significant contributions from the zero-point vibrational correction to the optical rotation, namely for **6**, **12** and **14**.[67] Also for other molecules, namely for tricycles, the vibrational corrections to the optical rotation have been found to be significant in earlier studies.[68] Nevertheless we did not include vibrational corrections in this study since from the work of Mort *et al.* it became clear that zero point vibrational corrections alone without inclusion of the solvent effects are not sufficient to improve the comparability between *ab initio* calculations and experiment.

In general CC2 behaves a little better than DFT. This is well demonstrated by performing linear regressions between the experimental values and the calculated ones according to

$$a = \frac{\sum_i [\alpha]_{\mathrm{theo},i} \cdot [\alpha]_{\mathrm{expt},i}}{\sum_i [\alpha]_{\mathrm{theo},i}^{\,2}}, \qquad (4)$$

where a is the linear regression parameter and $[\alpha]_{\mathrm{expt}}$ and $[\alpha]_{\mathrm{theo}}$ are the experimental and the calculated specific rotations, respectively. In Table 2 we have listed the linear regression parameters as well as their RMS errors calculated as

$$\Delta_{\mathrm{RMS}} = \sqrt{\frac{\sum_i \Delta_{\min}}{n}}, \qquad (5)$$

$$\Delta_{\min} = (a \cdot [\alpha]_{\mathrm{theo}} - [\alpha]_{\mathrm{expt}})^2, \qquad (6)$$

where n is the number of molecules in the test set. The deviation of a from 1 as well as the value of Δ_{RMS} can be taken as a measure of errors of a method in the reproduction of the experimental values. For B3LYP the regression parameter a deviates remarkably from 1 while CAM-B3LYP and CC2 give significantly better results of comparable accuracy if the DFT optimized geometries are used. Δ_{RMS}, which is a measure of scattering of the errors around the average factor a, is for CAM-B3LYP relatively high while for CC2 it is about 15% lower.

Only the CC2 results give a regression parameter close to 1 as well as a Δ_{RMS} in the range of 250. The parameters for the CC2 calculations show a remarkably low dependence on the basis set. More important is the influence of the geometry. Both the a parameter and Δ_{RMS} are significantly higher with MP2 than with DFT geometries. The largest contributions to Δ_{RMS} are from the group of large molecules in the test set, especially from the helicene derivatives which show deviations between theory and experiment in the range of several thousand deg $(\mathrm{dm\ g\ cm^{-3}})^{-1}$. Nevertheless it must be stated that also the absolute optical rotations of the helicene molecules are at least half an order of magnitude higher than the deviations. As discussed in more detail below, we observe a strong geometry-dependence of the optical rotation for the larger helicenes. It must be stressed that all experimental values given in Table 1 have been measured in solution or in neat liquids and according to our results we assume that there are significant differences between the helicene structures in solution and in the gas phase (*vide infra*) as well as between DFT and MP2 optimized geometries.

4.1 Sign reproduction

Since the comparison of calculated and measured optical rotations is used extensively to determine absolute configurations, the correct reproduction of the sign of the optical rotation is an important criterion for the validation of a theoretical method. In the test set are five molecules where the sign of the optical rotation differs between experiment and all calculations (**14**, **18**, **24**, **26** and **50**). In two other cases the sign differs among the calculated results (**6** and **28**). Apart from **6** all these molecules have also been considered to be problematic for sign determination by Stephens *et al.* in their 2005 study. Anyway, we must conclude that for sign determination CC2 does not offer an improvement.

In the cited work Stephens *et al.* have introduced a statistical technique to determine the reliability of quantum chemical methods for sign determination which defines a so-called ''zone of indeterminacy'' which is deduced from the RMS deviations between calculated and experimental values. Following the lines of Stephens *et al.* the width of the zone of indeterminacy Δ_{ZI} is determined as double the RMS error between the measured and calculated results. For our test set excluding the helicenes we did a corresponding analysis with the results listed in Table 3. Δ_{ZI} gives the minimum absolute value a theoretical optical rotation must have to obtain a sign determination with a reliability of 95%. For the determination of Δ_{ZI} we excluded the helicenes from the test set for which

Published on 09 January 2014. Downloaded by Ruhr Universitat Bochum on 07/07/2014 13:19:21.

Table 1 Calculated optical rotations for the molecules of the test set at 589 nm. All specific rotations are given in deg (dm g $cm^{-3})^{-1}$. All calculated values in columns 4–7 were obtained using geometries optimized with B3LYP/6-311(d,p) by Srebro and coworkers[6] if not stated otherwise. All results in column 8 have been obtained using an MP2/cc-pVTZ optimized geometry. Results marked† were obtained from B3LYP/6-31G* optimized geometries. B3LYP-results marked† were taken from ref. 30, all other B3LYP- and CAM-B3LYP-results were taken from ref. 6. All coupled cluster results have been obtained using the modified velocity gauge of Pedersen and coworkers[7]

					CC2, DFT geo.		
No.	Exp.	Ref.	B3LYP aug-cc-pVDZ	CAM-B3LYP aug-cc-pVDZ	aug-cc-pVDZ	aug-cc-pVTZ	CC2, MP2 geo. aug-cc-pVTZ
1	−18.77	31	−17.12	−22.30	−47.16	−36.04	−36.56
2	58.88	32	76.10	70.36	116.57	103.89	105.53
3	61.16	33	65.21	90.53	68.51	45.32	45.79
4	128.95	34	165.24	177.38	171.87	140.72	140.32
5	41.00	35	57.98	53.42	40.60	43.68	40.90
6	57.58	36	11.78	13.50	−0.31	−18.33	0.95
7	101.65	37	102.10	94.40	125.30	109.02	108.39
8	−16.77	37	−24.97	−43.85	−24.44	−29.59	−17.14
9	−1.33	37	−10.04	−25.79	−16.10	−20.32	−17.29
10	78.22	38	80.76	65.15	70.88	70.76	61.93
11	−103.34	38	−134.80	−142.01	−117.37	−121.96	−94.90
12	−34.50	39	−13.23	−23.85	−0.73	−4.02	−3.83
13	−37.07	39	−84.45	−88.13	−81.68	−85.85	−84.29
14	−27.23	40	8.46	4.17	3.65	3.75	4.56
15	−1145.72	41	−1193.81	−906.96	−801.38	−817.19	−890.00
16	59.12	42	58.36	37.68	56.36	56.15	56.29
17	−51.25	43	−66.08	−58.14	−62.58	−60.80	−55.68
18	6.60	44	−11.10†		−13.82†	−12.24†	−3.51
19	15.80	44	4.10†		6.58†	7.31†	13.24
20	−72.30	45	−56.70†		−61.66†	−58.30†	−56.33
21	−45.50	45	−28.90†		−25.99†	−25.81†	−24.54
22	46.60	46	32.80†		25.62†	35.60†	36.78
23	51.60	47	46.62	54.18	36.17	46.48	41.17
24	23.12	48	−25.52	−3.93	−24.70	−21.35	−19.43
25	−179.73	42	−253.69	−206.89	−244.58	−252.61	−273.21
26	7.24	42	−9.96	−10.54	−6.35	−5.74	−7.06
27	23.30	49	17.90†		8.08†	8.51†	10.83
28	−15.90	49	3.60†		−2.32†	−2.52†	−0.18
29	−286.80	50	−346.20	−215.06	−282.10	−283.64	−305.66
30	119.81	51	91.64	94.08	78.02	85.02	71.49
31	−2159.82	52	−2913.17	−2312.14	−2208.82	−2306.50	−2284.45
32	−3639.88	53	−4818.26	−3519.61	−3416.73	−3595.22	−2725.05
33	−3133.02	54	−6360.52	−4433.38	−4199.17	−4419.67	−3861.80
34	−3559.87	55	−4820.31	−3444.23	−3366.85	−3562.47	−3082.09
35	−6199.83	56	−6995.92	−4776.76	−4815.81	−5084.41	−4113.52
36	−175.59	57	−168.09	−156.20	−144.33	−143.26	−140.22
37	−33.56	58	−65.76	−67.58	−75.79	−49.77	−63.15
38	−21.16	59	−41.32	−45.14	−26.51	−26.82	−30.30
39	98.38	60	159.17	149.67	125.04	136.27	147.60
40	1.63	61	1.90	2.34	2.55	4.39	2.66
41	115.03	62	94.00	85.21	94.82	91.87	94.23
42	108.14	63	115.00	98.31	115.22	106.90	107.05
43	94.40	63	83.48	78.72	90.75	92.89	95.50
44	86.50	63	78.76	69.33	67.96	65.08	61.25
45	66.60	63	43.59	43.50	41.72	44.32	45.56
46	56.89	63	29.09	30.32	29.91	28.67	31.18
47	175.77	64	149.85	127.03	148.00	138.98	131.51
48	139.23	64	111.34	94.36	112.49	103.11	95.37
49	415.61	65	407.89	386.29	188.65	181.51	203.02
50	−78.40	66	13.20†		114.93†	87.81†	70.81

large absolute errors have been found which however correspond to very modest relative errors and show no problems in sign determination. In the cited study Stephens *et al.* found the width of the zone of determinacy for B3LYP to be 57.8 which is slightly below our value. Nevertheless we note that the test set Stephens *et al.* used has some similarities to our one (50% of the molecules of our test set are also contained in their test set) but it is 30% larger (50 *vs.* 65 molecules). However the worst offenders concerning sign determination are contained in both test sets. From our results we find that CC2 behaves much worse than DFT concerning sign determination. Comparing the results for the different geometries and basis sets we note that the influence of the geometry is much larger than the remaining basis set effects beyond aug-cc-pVDZ.

4.2 Influence of the geometry

The results of our calculations show that especially in the group of norbornane derivatives (**14–22**) and among the large molecules

 This journal is © the Owner Societies 2014

Published on 09 January 2014. Downloaded by Ruhr Universitat Bochum on 07/07/2014 13:19:21.

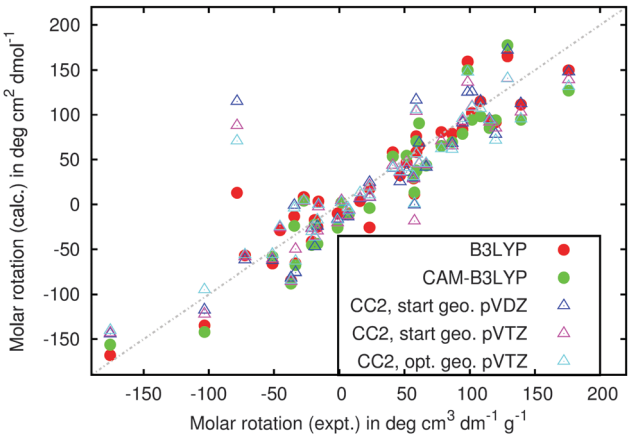


Fig. 6 Comparison of calculated and experimental results. All DFT results were calculated at the geometries from ref. 6 and 30, respectively. The coupled cluster-data marked "start geo." were also calculated at these geometries while the CC data marked "opt." were obtained at MP2 optimized geometries.

Table 2 Linear regression parameters and RMS deviations of the calculated values for the optical rotation shown in Table 1. The results marked† were calculated at MP2/cc-pVTZ optimized geometries. All other results are from geometries as stated in the caption of Table 1

	A	Δ_{RMS}
B3LYP, aug-cc-pVDZ	0.73	269
CAM-B3LYP, aug-cc-pVDZ	1.02	307
CC2, aug-cc-pVDZ	1.05	252
CC2, aug-cc-pVTZ	1.00	251
CC2, aug-cc-pVTZ‡	1.18	297

Table 3 Width of the "zone of indeterminacy" for our test set. The results marked‡ were calculated at MP2/cc-pVTZ optimized geometries. All other results are from geometries as stated in the caption of Table 1. For the determination of Δ_{ZI} the helicene derivatives **31–35** were excluded from the test set

	Δ_{ZI}
B3LYP, aug-cc-pVDZ	61.7
CAM-B3LYP, aug-cc-pVDZ	94.9
CC2, aug-cc-pVDZ	146
CC2, aug-cc-pVTZ	140
CC2, aug-cc-pVTZ‡	122.7

(**29–35**) the MP2/aug-cc-pVTZ results depend remarkably on the geometry. In these series of molecules the geometry effect often exceeds the basis set effect if we compare CC2/aug-cc-pVDZ and CC2/aug-cc-pVTZ results obtained with the geometries from the literature. Especially in the case of (1*S*,3*R*,4*R*)-*endo*-isocamphane (**18**) and (1*S*,3*S*,4*R*)-*exo*-isocamphane (**19**) we observe geometry effects which change the specific rotation (which is remarkably small for these molecules) by a factor of 4 or 2, respectively. In both cases the calculated results at the MP2 optimized structures are significantly closer to experiment than the others. A comparison of the MP2 geometries from the present work with the DFT geometries optimized by Crawford *et al.* reveals that for **18** and **19** the MP2 geometry has significantly shorter C–C bonds. The bond connecting the two methyl substituted carbon atoms is in both cases about 2 pm longer with B3LYP than with MP2. The reason for this is the dispersion interaction between the methyl groups which is not included in B3LYP. Similar observations are made for the optical rotations of (1*R*,2*S*,5*R*)-*cis*-pinane (**27**) and (1*S*,2*S*,5*S*)-*trans*-pinane (**28**) which are also fully saturated hydrocarbons without heteroatoms. The geometry effect is, however, for these molecules not as dramatic as for **18** and **19** but still exceeds by far the changes with the basis set.

4.3 Basis set effect

The basis set effect on the optical rotation can be estimated by comparing the two CC2 calculations which were carried out at the DFT geometries (6th and 7th columns in Table 1). The most remarkable basis set effects are found for the tricyclic molecules (**1–13**), especially for molecule **6**. Another molecule that shows a remarkable basis set effect is **50** which also belongs to the smaller members of the test set. We explain the higher sensitivity of the results for these molecules with their small size. Similar trends are known from polarizabilities and excitation energies where the basis set demands are usually higher for small molecules/chromophores than for large molecules/chromophores.

The significant basis set effect in **6** and **50** is illustrated by a series of calculations with the correlation consistent basis sets aug-cc-pV*X*Z with cardinal numbers *X* up to five. The basis set dependence of these two molecules is shown in Fig. 7 and Table 4. For both molecules the results get with increasing

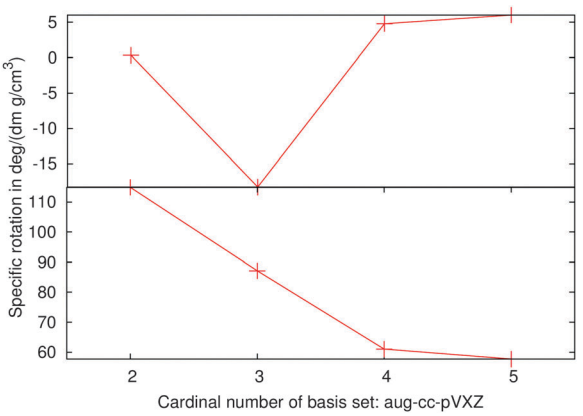


Fig. 7 Basis set behaviour of the molecules **6** (top) and **50** (bottom) of the test set.

Table 4 Basis set behaviour of **6** and **50**. The experimental values are repeated for comparison. All values are given in deg (dm g cm^{-3})$^{-1}$. Calculations were performed using CC2 and the MP2/cc-pVTZ optimized geometry

	6	**50**
aug-cc-pVDZ	0.31	114.9
aug-cc-pVTZ	−18.3	87.1
aug-cc-pVQZ	4.77	61.0
aug-cc-pV5Z	6.01	57.7
Expt.	57.58	−78.4

Published on 09 January 2014. Downloaded by Ruhr Universitat Bochum on 07/07/2014 13:19:21.

cardinal number closer to the experimental value. Nevertheless, even for aug-cc-pV5Z the optical rotation is far from being in accordance with experiment.

4.4 Spin scaling effects

Due to the encouraging results that have been obtained by applying Grimme's spin scaling technique for MP2[69] and CC2[70] in the calculation of reaction energies and the optimization of molecular geometries we applied spin-component scaled CC2 (SCS-CC2) in the current work for the calculation of optical rotations. The results for a part of the test set are shown in Table 5. They show that spin scaling does not offer any improvement concerning the deviation between theory and experiment. In most cases experimental values are reproduced better without use of spin scaling. In some cases (see *e.g.* **8**, **12** and **50**) spin scaling can change the optical rotation by a factor of more than two.

Table 5 Calculated optical rotations for the molecules **1–28** using spin-component scaled CC2. All calculations have been carried out on a geometry which was optimized using MP2 and cc-pVTZ. The experimental values and the results from regular CC2 at the same geometry are the same as in Table 1 and are repeated for comparison

No.	Exp.	Ref.	CC2	SCS-CC2
1	−18.77	31	−36.56	−25.38
2	58.88	32	105.53	58.26
3	61.16	33	45.79	40.40
4	128.95	34	140.32	123.45
5	41.00	35	40.90	56.73
6	57.58	36	0.95	−40.73
7	101.65	37	108.39	89.85
8	−16.77	37	−17.14	−36.51
9	−1.33	37	−17.29	−27.71
10	78.22	38	61.93	48.94
11	−103.34	38	−94.90	−110.59
12	−34.50	39	−3.83	−19.06
13	−37.07	39	−84.29	−88.70
14	−27.23	40	4.56	−14.05
15	−1145.72	41	−890.00	−610.36
16	59.12	42	56.29	35.60
17	−51.25	43	−55.68	−60.66
18	6.60	44	−3.51	−3.96
19	15.80	44	13.24	14.71
20	−72.30	45	−56.33	−69.61
21	−45.50	45	−24.54	−35.67
22	46.60	46	36.78	41.60
23	51.60	47	41.17	63.68
24	23.12	48	−19.43	−1.06
25	−179.73	42	−273.21	−217.53
26	7.24	42	−7.06	−12.76
27	23.30	49	10.83	8.79
28	−15.90	49	−0.18	4.12
36	−175.59	57	−140.22	−131.60
37	−33.56	58	−63.15	−47.53
38	−21.16	59	−30.30	44.89
39	98.38	60	147.60	164.76
40	1.63	61	2.66	2.47
41	115.03	62	94.23	84.20
42	108.14	63	107.05	92.17
43	94.40	63	95.50	88.65
44	86.50	63	61.25	60.26
45	66.60	63	45.56	46.77
46	56.89	63	31.18	29.95
47	175.77	64	131.51	113.11
48	139.23	64	954.37	82.61
49	415.61	65	203.02	232.06
50	−78.40	66	70.81	30.97

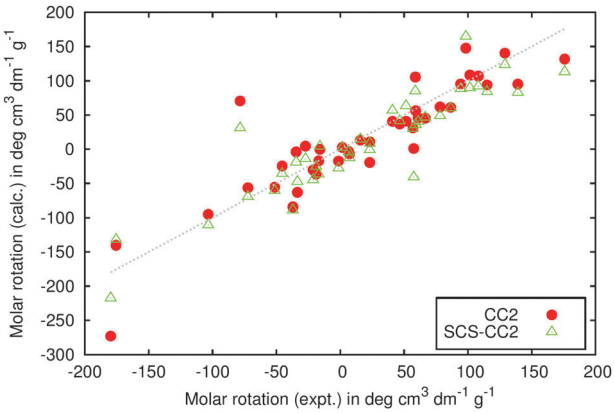


Fig. 8 Comparison of CC2- and SCS-CC2 results to experimental values.

Comparing these findings to our results for isotropic polarizabilities[71] and vibrational frequencies[22] we note that at first sight the effects of spin scaling seem to be larger for the optical rotation. One should, however, take into account that the optical rotation is an anisotropic property which even for large molecules can be accidentally small due to a cancellation of different contributions. Anyway, apart from reaction energies, the most significant improvements by spin-component scaling have been observed for geometries. Therefore a comparison of optical rotations calculated with CC2 at SCS-MP2 optimized geometries would make sense if gas-phase data for optical rotations would be available for a sufficiently large test set. A graphical comparison of the CC2 and SCS-CC2 results with the experimental values is shown in Fig. 8.

4.5 Helicenes

In addition to the helicene derivatives **31–35** from the test set we also calculated optical rotations of four larger helicene derivatives at geometries optimized at the DFT and MP2 level. For comparability with the results of the smaller helicenes we followed for the DFT calculations Srebro *et al.* and used the 6-311G* basis set combined with the B3-LYP functional while the MP2 optimizations were done with the cc-pVTZ basis.

The geometries optimized with MP2 are more compact than those from B3LYP, which is related to the (intramolecular) dispersion interaction between the π-stacked benzene rings which is neglected by B3LYP and overestimated by MP2 according to the findings of Ehrlich and coworkers.[72] This could also explain the rather large difference between measured and calculated values of the helicenes at the MP2 geometries since the interaction between the molecule and the solvent (which was $CHCl_3$ in most cases) could result in similar effects on the structure as the change in the electronic structure method. A measure of the deviation of the structures is the difference in the dihedral angles between the carbon atoms of the inner helix, defined as illustrated in Fig. 9, which are listed in Table 6.

The calculated values of the helicene molecules are listed in Table 7. In Fig. 10 we give a graphical comparison of calculated and experimental values of the optical rotation of the helicenes with 5 to 11 rings. This plot shows two remarkable features.

 This journal is © the Owner Societies 2014

Published on 09 January 2014. Downloaded by Ruhr Universitat Bochum on 07/07/2014 13:19:21.

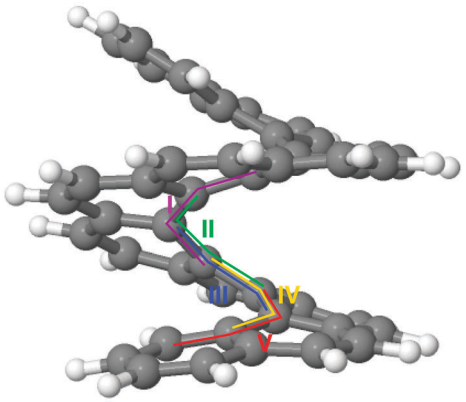


Fig. 9 Dihedral angles in 11-helicene.

Table 6 Behaviour of the dihedral angles in different helicene structures. The numbers of the angles follow the numbers in Fig. 9

Helicene	Method	I	II	III	IV	V
5	DFT	30.1	18.1			
	MP2	29.6	18.3			
6	DFT	28.9	13.8			
	MP2	26.1	16.2			
7	DFT	28.2	25.5	16.5		
	MP2	22.0	24.2	21.5		
8	DFT	25.5	28.0	16.5		
	MP2	22.7	25.2	19.5		
9	DFT	22.8	27.8	28.0	14.8	
	MP2	23.0	24.8	25.5	18.5	
10	DFT	26.3	27.1	26.6	15.6	
	MP2	25.2	23.7	24.6	19.4	
11	DFT	28.7	25.6	26.5	27.1	15.7
	MP2	27.1	24.2	22.9	25.6	19.1

Table 7 Results for the helicene molecules from different methods. Results marked‡ were taken from ref. 6. Experimental values for the helicenes with more than seven rings are taken from ref. 73

				CC2	
				Structure	
Helicene	Expt.	B3LYP	CAM-B3LYP	DFT	MP2
5	−2160	−2913‡	−2312‡	−2209	−2189
6	−3640	−4818‡	−3519‡	−3417	−2725
7	−6200	−6996‡	−4777‡	−4816	−3828
8	−6690	−8888		−6018	−4535
9	−7500	−10 394		−6997	−4757
10	−8300	−11 887		−7836	−4737
11		−12 823		−8355	−4613

First of all, the experimental values are overestimated significantly by the B3YLP calculations while the other methods more or less underestimate the optical rotation. Secondly, we note that the CC2 results for the MP2 structures are far off the experimental values and that their absolute values do not increase monotonically but reach a maximum value with nine rings and decrease thereafter.

Anyway, the experimental values are better reproduced by CC2 and CAM-B3LYP for all helicenes apart from 7-helicene where the B3LYP result is closer to the experimental result.

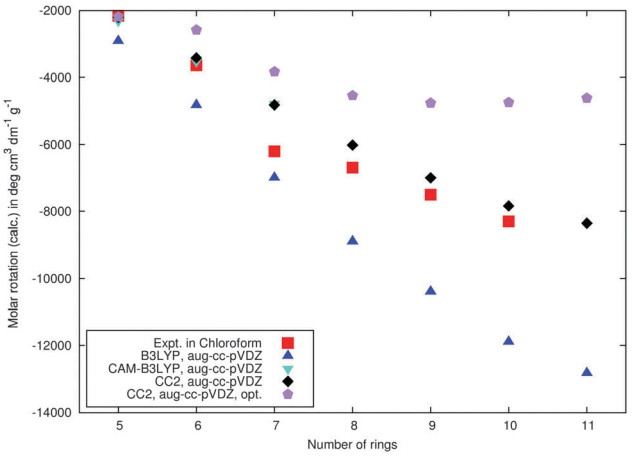


Fig. 10 Comparison of calculated and experimental results for helicenes. All results for the 5-, 6- and 7-helicenes were calculated at the geometries from ref. 6 if not stated otherwise. The results for the 8-, 9-, 10- and 11-helicenes were calculated at DFT geometries obtained in the current work with the B3LYP functional and the 6-311G(p,d) basis, if not stated otherwise. The coupled cluster data marked with "opt." were obtained at MP2/cc-pVTZ geometries.

On the whole, 7-helicene plays a special role in the series of helicenes that we investigated here as it marks some kind of discontinuity in the plot of the experimental values in Fig. 10 as well as in the behaviour of the dihedral angles which differ severely between the MP2 and B3LYP geometries for this molecule. We suppose that this is related to the fact that 7-helicene is the first member of the *n*-helicenes with π-stacked benzene rings. In the 5- and 6-helicene the two ends of the helix do not yet overlap so that there are no π-stacking interactions.

MP2 is known to overestimate dispersion interactions in π-stacked structures. Ehrlich *et al.* found recently[72] that for large acenes with intramolecular π-stacking interactions this can lead to non-negligible errors in geometries. The comparison of our calculations with the experimental data is also impaired by the fact that the measurements[73] of the helicenes have been done in solution, where the interaction with the solvent competes with the intramolecular π-stacking interactions and probably expands the helicene compared to the gas phase structures. For the B3LYP geometries this leads to a partial cancellation of the errors caused by the neglect of the intramolecular dispersion interaction and the solvent effects. Similar findings have been made by Srebro *et al.* who have compared calculated optical rotations for DFT geometries which were obtained with and without dispersion correction and different long-range correction parameters.[74] Srebro *et al.* assume that the structures obtained with corrected DFT represent better the gas-phase structures while the experimental values which are used for comparison were found for structures in the condensed phase. Due to these findings it appears to us that for the prediction of optical rotations of helicenes currently the best choice is to use CC2 in combination with DFT geometries, until a more accurate but efficient electronic structure method for geometry optimizations of systems with strong π-stacking interactions in solution is available.

Published on 09 January 2014. Downloaded by Ruhr Universitat Bochum on 07/07/2014 13:19:21.

5 Conclusion

We presented calculations of the optical rotation for a set of 50 molecules that have been studied previously using other methods. The test set contains molecules with up to 48 atoms that cover a wide range of optical rotations. The treatment of molecules as large as 11-helicene by a coupled cluster method became possible by the RI approximation for the two-electron integrals and an MPI parallelization. Origin independence is achieved through the modified velocity gauge formulation proposed by Pedersen.[7] The optical rotations were calculated with CC2 in augmented correlation-consistent basis sets at geometries optimized either with DFT or MP2. Compared to DFT we do not observe a large systematic improvement for CC2 concerning the agreement with the experimental data, although the scattering of the CC2 values around the regression curve is smaller than for DFT.

Comparing the results with DFT and MP2 structures we find that for helicenes the optical rotation shows a significant dependence on the geometry. For the helicene derivatives the structures from MP2 have been found to be much more compact than those from DFT because of the different description of the intramolecular dispersion interaction. For most of these large molecules the CC2 results reproduce the experimental data better than the results from DFT while we found that the results obtained with MP2 structures are very far from both experimental results and values obtained with DFT structures. Therefore the use of CC2 with DFT structures has proven to be very recommendable to treat the optical rotation of helicenes.

Concerning the correct sign prediction we must state that CC2 behaves worse than DFT for the test set we used and also in comparison to an earlier study by Stephens and coworkers.[5] The reproduction of the correct sign has turned out to be difficult for five molecules from the test set which are known to be problematic.[5] The use of the spin scaling technique which has proven to be a reasonable correction *e.g.* for geometries in CC2 and MP2 results offers no benefit concerning optical rotation calculations.

Regarding all these results we conclude that CC2 may not be an improvement for the treatment of "unproblematic" molecules. Nevertheless the test calculations especially of the helicene molecules have shown that the RI-CC2 approach is an efficient tool to calculate optical rotations of systems which are influenced by inter- or intramolecular dispersion interactions and π-stacking effects. For these it outperforms density functional methods.

Acknowledgements

The authors acknowledge support from the Deutsche Forschungsgemeinschaft (DFG) through grant HA 2588/5-1.

References

1 T. B. Freedman, X. Cao, R. K. Dukor and L. A. Nafie, *Chirality*, 2003, **15**, 743–758.
2 J. R. Cheeseman, M. J. Frisch, F. J. Devlin and P. J. Stephens, *J. Phys. Chem. A*, 2000, **104**, 1039–1046.
3 P. Stephens, D. McCann, J. Cheeseman and M. Frisch, *Chirality*, 2005, **17**, S52–S64.
4 P. J. Stephens, F. J. Devlin, C. F. Chabalowski and M. J. Frisch, *J. Phys. Chem.*, 1994, **98**, 11623–11627.
5 P. J. Stephens, F. J. Devlin, J. R. Cheeseman and M. J. Frisch, *J. Phys. Chem. A*, 2001, **105**, 5356–5371.
6 M. Srebro, N. Govind, W. A. de Jong and J. Autschbach, *J. Phys. Chem. A*, 2011, **115**, 10930–10949.
7 T. B. Pedersen, H. Koch, L. Boman and A. M. Snchez de Meras, *Chem. Phys. Lett.*, 2004, **393**, 319–326.
8 F. London, *J. Phys. Radium*, 1937, **8**, 397.
9 T. Helgaker and P. Jørgensen, *J. Chem. Phys.*, 1991, **95**, 2595–2601.
10 T. B. Pedersen and H. Koch, *J. Chem. Phys.*, 1997, **106**, 8059–8072.
11 T. B. Pedersen, H. Koch and K. Ruud, *J. Chem. Phys.*, 1999, **110**, 2883–2892.
12 T. B. Pedersen and H. Koch, *J. Chem. Phys.*, 2000, **112**, 2139–2147.
13 T. B. Pedersen, B. Fernández and H. Koch, *J. Chem. Phys.*, 2001, **114**, 6983–6993.
14 K. Ruud, P. J. Stephens, F. J. Devlin, P. R. Taylor, J. R. Cheeseman and M. J. Frisch, *Chem. Phys. Lett.*, 2003, **373**, 606–614.
15 T. B. Pedersen, A. M. J. S. Sánchez de Meras and H. Koch, *J. Chem. Phys.*, 2004, **120**, 8887–8897.
16 O. Christiansen, H. Koch and P. Jørgensen, *Chem. Phys. Lett.*, 1995, **243**, 409–418.
17 C. Hättig and F. Weigend, *J. Chem. Phys.*, 2000, **113**, 5154–5161.
18 C. Hättig and A. Köhn, *J. Chem. Phys.*, 2002, **117**, 6939–6951.
19 A. Köhn and C. Hättig, *J. Chem. Phys.*, 2003, **119**, 5021–5036.
20 C. Hättig and P. Jørgensen, *J. Chem. Phys.*, 1998, **109**, 2762–2778.
21 D. H. Friese, N. O. C. Winter, P. Balzerowski, R. Schwan and C. Hättig, *J. Chem. Phys.*, 2012, **136**, 174106.
22 D. H. Friese, C. Hättig and J. Koßmann, *J. Chem. Theor. Comput.*, 2013, **9**, 1469–1480.
23 J. Linderberg and Y. Öhrn, *Propagators in Quantum Chemisty*, Academic, 1973.
24 *TURBOMOLE developer's version, a devolpment of Universität Karlsruhe and of Forschungszentrums Karlsruhe GmbH, 1989–2007, TURBOMOLE GmbH, 2007; available at* http://www.turbomole.com.
25 T. H. Dunning, *J. Chem. Phys.*, 1989, **90**, 1007–1023.
26 D. E. Woon and T. H. Dunning, *J. Chem. Phys.*, 1993, **98**, 1358–1371.
27 F. Weigend, A. Köhn and C. Hättig, *J. Chem. Phys.*, 2002, **116**, 3175–3183.
28 C. Hättig, *Phys. Chem. Chem. Phys.*, 2005, **7**, 59–66.
29 K. A. Peterson, D. Figgen, E. Goll, H. Stoll and M. Dolg, *J. Chem. Phys.*, 2003, **119**, 11113–11123.
30 T. D. Crawford and P. J. Stephens, *J. Phys. Chem. A*, 2008, **112**, 1339–1345.
31 Y. Kumata, J. Furukawa and T. Fueno, *Bull. Chem. Soc. Jpn.*, 1970, **43**, 3920–3921.
32 V. Schurig, B. Koppenhoefer and W. Buerkle, *J. Org. Chem.*, 1980, **45**, 538–541.

 This journal is © the Owner Societies 2014

Published on 09 January 2014. Downloaded by Ruhr Universitat Bochum on 07/07/2014 13:19:21.

33 T. Tsunetsugu, J. Furukawa and T. Fueno, *J. Polym. Sci., Part A-1: Polym. Chem.*, 1971, **9**, 3529–3540.
34 G. Helmkamp and N. Schnautz, *Tetrahedron*, 1958, **2**, 304–307.
35 W. R. Moore, H. W. Anderson, S. D. Clark and T. M. Ozretich, *J. Am. Chem. Soc.*, 1971, **93**, 4932–4934.
36 J. J. Gajewski, *J. Am. Chem. Soc.*, 1971, **93**, 4450–4458.
37 G. V. Shustov, A. V. Kachanov, V. A. Korneev, R. G. Kostyanovsky and A. Rauk, *J. Am. Chem. Soc.*, 1993, **115**, 10267–10274.
38 G. V. Shustov, G. K. Kadorkina, R. G. Kostyanovskii and A. Rauk, *J. Am. Chem. Soc.*, 1988, **110**, 1719–1726.
39 W. H. Pirkle and P. L. Rinaldi, *J. Org. Chem.*, 1977, **42**, 3217–3219.
40 E. Plettner, A. Mohle, M. T. Mwangi, J. Griscti, B. O. Patrick, R. Nair, R. J. Batchelor and F. Einstein, *Tetrahedron: Asymmetry*, 2005, **16**, 2754–2763.
41 D. A. Lightner, J. K. Gawronski and T. D. Bouman, *J. Am. Chem. Soc.*, 1980, **102**, 5749–5754.
42 E. Giorgio, R. G. Viglione, R. Zanasi and C. Rosini, *J. Am. Chem. Soc.*, 2004, **126**, 12968–12976.
43 W. M. D. Wijekoon, E. Bunnenberg, R. Records and D. A. Lightner, *J. Phys. Chem.*, 1983, **87**, 3034–3037.
44 A. A. Vereshchagina, T. I. Sapteeva, L. G. Slivkin, V. I. Garmashov and G. A. Rudakov, *J. Appl. Chem. USSR*, 1982, **55**, 409.
45 P. V. Ramachandran, G.-M. Chen and H. C. Brown, *J. Org. Chem.*, 1996, **61**, 88–94.
46 M. Nakazaki, K. Naemura and Y. Kondo, *J. Org. Chem.*, 1979, **44**, 16–20.
47 W. S. Johnson, B. Frei and A. S. Gopalan, *J. Org. Chem.*, 1981, **46**, 1512–1513.
48 H. C. Brown, M. Zaidlewicz and K. S. Bhat, *J. Org. Chem.*, 1989, **54**, 1764–1766.
49 G. Zweifel and H. C. Brown, *J. Am. Chem. Soc.*, 1964, **86**, 393–397.
50 S. H. Wilen, J. Z. Qi and P. G. Williard, *J. Org. Chem.*, 1991, **56**, 485–487.
51 H. B. Henbest and W. R. Jackson, *J. Chem. Soc.*, 1962, 954–959.
52 H. J. Bestmann and W. Both, *Chem. Ber.*, 1974, **107**, 2926–2930.
53 M. S. Newman, W. B. Lutz and D. Lednicer, *J. Am. Chem. Soc.*, 1955, **77**, 3420–3421.
54 E. Anger, M. Srebro, N. Vanthuyne, L. Toupet, S. Rigaut, C. Roussel, J. Autschbach, J. Crassous and R. Rau, *J. Am. Chem. Soc.*, 2012, **134**, 15628–15631.
55 D. A. Lightner, D. T. Hefelfinger, T. W. Powers, G. W. Frank and K. N. Trueblood, *J. Am. Chem. Soc.*, 1972, **94**, 3492–3497.
56 R. Martin, M. Flammang-Barbieux, J. Cosyn and M. Gelbcke, *Tetrahedron Lett.*, 1968, **9**, 3507–3510.
57 R. Rossi and P. Diversi, *Tetrahedron*, 1970, **26**, 5033–5039.
58 M. Segi, M. Takebe, S. Masuda, T. Nakajima and S. Suga, *Bull. Chem. Soc. Jpn.*, 1982, **55**, 167–170.
59 L. A. Paquette and J. P. Freeman, *J. Org. Chem.*, 1970, **35**, 2249–2253.
60 D. J. Pasto and K. D. Sugi, *J. Org. Chem.*, 1991, **56**, 4157–4160.
61 J. Canceill, L. Lacombe and A. Collet, *J. Am. Chem. Soc.*, 1985, **107**, 6993–6996.
62 J. Pecka and M. Cerny, *Collect. Czech. Chem. Commun.*, 1973, **38**, 132–142.
63 N. Ibrahim, T. Eggimann, E. Dixon and H. Wieser, *Tetrahedron*, 1990, **46**, 1503–1514.
64 A. E. Wroblewski, J. Applequist, A. Takaya, R. Honzatko, S. S. Kim, R. A. Jacobson, B. H. Reitsma, E. S. Yeung and J. G. Verkade, *J. Am. Chem. Soc.*, 1988, **110**, 4144–4150.
65 M. G. Mason and O. Schnepp, *J. Chem. Phys.*, 1973, **59**, 1092–1098.
66 M. Nakazaki, K. Naemura and N. Arashiba, *J. Org. Chem.*, 1978, **43**, 888–891.
67 B. C. Mort and J. Autschbach, *J. Phys. Chem. A*, 2005, **109**, 8617–8623.
68 K. Ruud, P. R. Taylor and P.-O. A. strand, *Chem. Phys. Lett.*, 2001, **337**, 217–223.
69 S. Grimme, *J. Chem. Phys.*, 2003, **118**, 9095–9102.
70 A. Hellweg, S. A. Grün and C. Hättig, *Phys. Chem. Chem. Phys.*, 2008, **10**, 4119–4127.
71 D. H. Friese, PhD thesis, Ruhr-Universität Bochum, 2012.
72 S. Ehrlich, H. F. Bettinger and S. Grimme, *Angew. Chem., Int. Ed.*, 2013, **52**, 10892–10895.
73 R. H. Martin and V. J. Libort, *J. Chem. Res.*, 1980, **4**, 1940–1950.
74 M. Srebro and J. Autschbach, *J. Chem. Theor. Comput.*, 2012, **8**, 245–256.